

A new numerical technique for tracking chemical species in a multisource, coastal ecosystem applied to nitrogen causing *Ulva* blooms in the Bay of Brest (France)

Alain Ménesguen¹ and Philippe Cugier

Département d'Ecologie Côtière, Direction de l'Environnement et de l'Aménagement Littoral, IFREMER/Centre de Brest, 29280 Plouzané, France

Isabelle Leblond

Laboratoire E312, ENSIETA, 2 rue François Verny, 29806 Brest Cedex 09, France

Abstract

A new numerical technique is presented that allows the tracking of any chemical element from any source in a simulated foodweb, for instance assessing the proportion of these sources (river loadings, sea entrances, point sources) in the algal diet for the limiting nutrient. An application is shown for nitrogen in an *Ulva* bloom occurring in a shallow embayment connected with a strongly tidally stirred ecosystem with various sources of inorganic nitrogen, the Bay of Brest, Brittany, France. In a first step, a biogeochemical three-dimensional model was developed to simulate growth and erosion–transport–deposition of free-floating ulvae; this model was able to converge on a realistic distribution of *Ulva* deposits after a few months, even though it was initialized with a strongly unrealistic distribution of settled ulvae. In a second step, and unfortunately for recovery plans, the tracking technique, applied in this model to all the nitrogen sources entering the bay, revealed that the small, nitrate-polluted rivers flowing directly into the eutrophicated area had a negligible effect, whereas more distant but stronger sources, a big river and a big urban sewage plant, even after dilution, accounted for about 50% and 20%, respectively, of the algal nitrogen content during summer. Despite its high N flux, open ocean contributes only 15% to *Ulva* growth. The suppression of only one of the main nitrogen sources would not significantly decrease the *Ulva* bloom, because of the high nitrogen surplus present in the site. The remaining sources would still saturate the needs of the maximum *Ulva* biomass the site is able to produce. The tracking technique, however, shows that the N turnover in *Ulva* is only 4 months. Thus, improvements would occur within a year following large N reductions.

Eutrophication has been of increasing concern for a while, first in lakes and rivers, and then in the coastal zone. Many studies have been done to point out which nutrient was the limiting or the controlling one in various eutrophicated water bodies: whereas phosphorus has been recognized for a long time as the limiting factor in most polluted freshwater systems (Vollenweider 1968; Schindler 1975), a more contrasted situation arose in coastal marine environments. Phytoplanktonic massive blooms in the plumes of main rivers are rather phosphorus- or silicon-limited near shore, but nitrogen-limited off shore, especially in summer. The continuously changing N:P:Si ratio in enriched coastal waters may

drastically change the conclusions about the controlling factor in a few years (Guillaud et al. 2000). Green macrophyte blooms, on the contrary, were unanimously considered as being always nitrogen controlled. This form of eutrophication is typical of coastal, very shallow areas that have been heavily enriched in inorganic nitrogen, mainly of land runoff origin (nitrate), but sometimes of urban sewage origin (ammonia or nitrate). Both for phytoplankton and macrophytes, when the limiting factor has been well established, the question often arises about the main source to be diminished: operational restoring plans need to identify the most important target, and to know to what extent the nutrient load has to be reduced. Direct field experiments with chemical tracers are unfeasible in many cases, because of the nonexistence of enough isotopes of the element under study (a n-source problem requires at least $n - 1$ isotopes), or the absence of sufficient discrepancy between the natural isotopic signatures of the various sources. Only numerical models can evaluate the effect of each source on the global system, but, up to now, they have been used to test modified situations, e.g., partial or total removal of a nutrient source. This paper shows how to track separately, in the whole, undisturbed, simulated food web, the limiting element coming from a specific input in a multisource context, and to assess the precise proportion of the different existing sources in the actual feeding of proliferating algae. Application of the technique has been done in the case of an *Ulva* mass bloom arising in a small embayment communicating with a highly mixed tidal ecosystem with many sources of inorganic nitrogen.

¹ Corresponding author (amenesg@ifremer.fr).

Acknowledgments

We thank our IFREMER's colleague Jacky L'Yavanc, who performed the survey for fine-scale bathymetry of the area of interest, and the municipal analysis laboratory of Brest ("Pôle Analytique des Eaux," belonging to the European Economic Interest Group "Littoralis," specializing in integrated Coastal-Zone Management) for all the nutrient concentrations measured in tributaries. We also thank the CEVA laboratory for providing the map of its diver-operated survey of submersed *Ulva* deposits, and the so-called "SOM-LIT-Iroise" team of the French Monitoring Service of the INSU-CNRS, who kindly provided the 1999 time-series of hydrological data at the Sainte-Anne station. The manuscript was substantially improved thanks to remarks provided by the two reviewers and the editor in chief.

This study has been granted by the Brest municipality (Brittany, France).

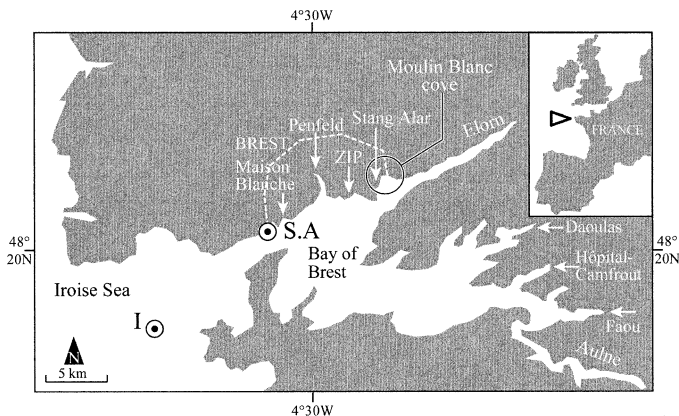


Fig. 1. Map of the Bay of Brest, with location of the main tributaries and of the marine stations Iroise (I) and Sainte-Anne (S.A.).

Materials and methods

Site description—The Bay of Brest, a rather small (180 km²) but productive region of freshwater influence, is situated at the western end of Brittany, France (Fig. 1). It has been intensively studied during the last 30 yr, partly because it represents in a certain sense an extreme estuarine situation, with very high nutrient loadings flowing into a very dispersive macrotidal marine ecosystem. The two main tributaries (Aulne and Elorn Rivers) drain a 2,800 km²-wide watershed, supporting a rather scattered population (360,000 inhabitants) but a highly intensive agricultural activity, mostly cattle breeding. As a result, Aulne and Elorn Rivers exhibit very high nitrate-specific fluxes (i.e., per watershed surface unit), which can be considered as maximum values in the whole North Atlantic region: Aurousseau (2001) gives for the Elorn River during the exceptionally rainy year 2000 a maximum annual specific flux of 9,500 kg km⁻² yr⁻¹ N; and a mean annual specific flux during recent years of 7,200 kg km⁻² yr⁻¹ N for the Elorn River and 5,000 kg km⁻² yr⁻¹ N for the Aulne river. These values are very high compared to the 1,450 kg km⁻² yr⁻¹ N value for the Seine + Rhine + Elbe ensemble and the 600 kg km⁻² yr⁻¹ N overall North Atlantic mean computed by Howarth et al. (1996). At the

end of the 20th century, the corresponding nitrogen loadings amounted to about 2.7×10^6 kg yr⁻¹ N for the Elorn River and to 8.6×10^6 kg yr⁻¹ N for the Aulne River. Apart from these two main rivers, the Bay of Brest receives six small other rivers, and two main urban sewage plants; all these tributaries are located on Fig. 1, and their annual mean flow rates as well as their mean nitrate, ammonia, and phosphate concentrations during the year 1999 are given in Table 1. Comparatively, and because of the prevailing westerlies coming directly from the North Atlantic Ocean, atmospheric nitrogen inputs are very low in the Bay of Brest, about 80×10^3 kg yr⁻¹ (Souchu 1986); they will be neglected in this study.

These high nitrogen loadings into a semienclosed bay could be thought to induce a critical eutrophicated status, which is really not the case today. This paradoxical situation has been described and explained by Le Pape et al. (1996) and Le Pape and Ménesguen (1997) as a consequence of the very intense vertical and horizontal mixing by tides (mean amplitude 4 m, spring tide amplitude 7.5 m), which disperse nutrients and growing phytoplankton into a wide and locally deep (up to 40 m) water volume, regularly exchanging with the open sea at its western hydrodynamical margin (the so-called Iroise Sea on Fig. 1). Nevertheless, apart from the general good health status of the central Bay of Brest, some peripheral and confined eutrophication phenomena have been recorded for several years, which are restricted to estuaries proper (e.g., *Prorocentrum micans* red-brown waters in summer at the mouth of Elorn River) or to embayments somewhat disconnected from the central intense tidal circulation. The most typical one is a “green tide,” made of free-floating *Ulva rotundata*, which grow and settle in the shallow Moulin Blanc cove, containing both the Brest beach and yachting port (Fig 2). Annual statistics from the Brest public utilities, which give the annual volume of ulvae collected by bulldozers on the beach, reveal a rather stable biomass production of the site: from 1989 until 1999, the annually collected volume fluctuated between 635 m³ and 1,694 m³, with a mean of 1,048 m³. To reduce this nuisance, the Brest municipality launched in 1999 a targeted action aiming at making an inventory of all the potential causes of

Table 1. Mean annual flow rates of the tributaries and their mean annual ammonia, nitrate, phosphate, and silicate concentrations for year 1999.

	Flow rate (m ³ s ⁻¹)	[NH ₄] (μmol L ⁻¹)	[NO ₃] (μmol L ⁻¹)	[PO ₄] (μmol L ⁻¹)	[Si(OH) ₄] (μmol L ⁻¹)
Elorn river	8.1	6.6	646.6	2.7	141.5
Aulne river	33.7	3.2	412.8	1.3	113.9
Penfeld river	0.7	2.5	631.5	2.7	231.5
Stang Alar river	0.1	5	514.2	2.8	140
Costour river	0.1	5	714.2	2.8	140
Daoulas, Hôpital-Camfrout & Faou rivers	~1.7 each	3.6	398.4	1.1	113.9
Zone Industrielle Portuaire (ZIP) & Maison-Blanche sewage plants	0.3 each	1890	56.8	297	140
Iroise Sea	11,000 (neap tide) 33,000 (spring tide)	0.4	4.4	0.2	2.9

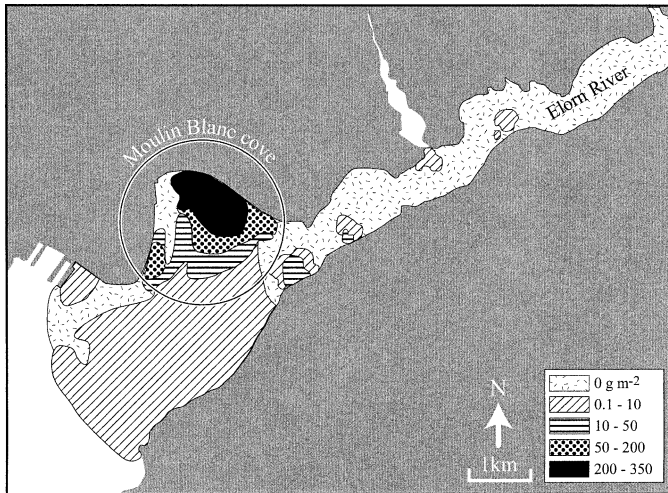


Fig. 2. Map of submerged benthic deposits of free ulvae, in June 2000 (from CEVA 2000).

this *Ulva* bloom, with a particular interest in identifying the main nutrient sources feeding the algae. In June 2000, a diver-operated survey was conducted by the CEVA lab (CEVA 2000), providing the map of submerged bottom deposits of ulvae in the whole Elorn estuarine area (Fig. 2). The work detailed hereafter consisted in building a mathematical model of algal primary production in the Bay of Brest, able to explain in a robust fashion the actual location and biomass of this very restricted algal mass bloom, and to assess the respective roles of the various tributaries in this eutrophication process.

Model equations—The three-dimensional (3D) ecological model is based on the phytoplankton model previously applied to the Bay of Seine area and described elsewhere (Cugier et al. 2005), adapted to the Bay of Brest problem by adding *Ulva* equations modified from Ménesguen and Salomon (1988) and Ménesguen (1992).

Model of the physical environment—The hydrodynamical context is furnished by SiAM3D model (Cugier and Le Hir 2002), a 3D hydrodynamic model that solves the so-called “shallow water” equations, using a finite difference technique on a nonuniform rectangular horizontal computational grid. As shown in Fig. 3, this allows one to define small meshes in an area of interest, for instance here the Elorn estuary and its eutrophicated cove (mesh size = 150 m), while keeping large meshes in far regions (mesh size = 1,000 m at the western entrance of the Bay). The model provides water surface elevation and velocities in the three space directions at each node of the grid, and solves an advection–dispersion equation for temperature (X_T), salinity (X_S), inorganic suspended matter (X_{SM}), and, more generally, any dissolved or particulate variable. The model uses real depth coordinates on the vertical axis, which is split into a maximum of 10 layers of given thickness (2 m for the four layers above the zero hydrographic level, 3 m, 3 m, 4 m, 5 m, 10 m, and up to 20 m beneath) as explained in Fig. 4. The model is forced with tidal harmonic components at the

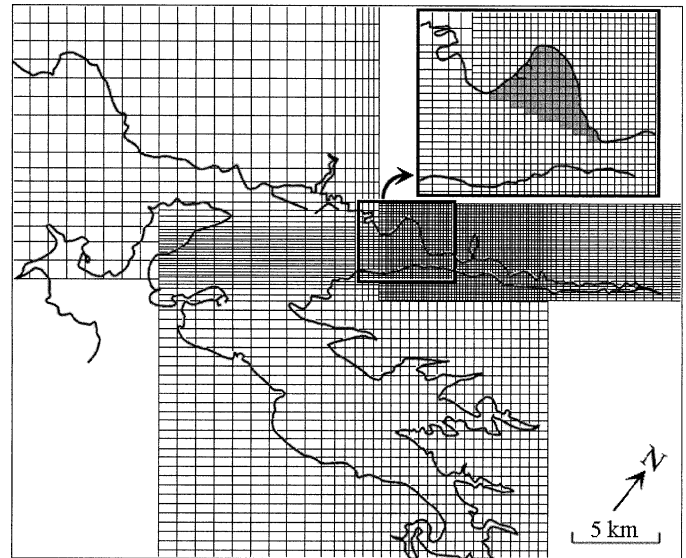


Fig. 3. Rectangular nonuniform grid used for the model (inset: in gray, area retained for summation of *Ulva* deposits in the Moulin Blanc cove).

marine boundaries, with measured flows and concentrations at river boundaries and with wind-induced stresses at the surface. The two main tributaries (Elorn and Aulne Rivers) were meshed up to their upstream tidal limit propagation, but the six other small rivers and two sewage outlets were considered as simple freshwater inputs in the marine meshes containing their outlet. The model also takes into account one or several sediment layers. Bottom exchanges are formulated according to Partheniades for erosion and to Krone for deposition (Cugier and Le Hir 2000).

Harmonic components of tide at the sea boundary and bathymetry were provided by the Service Hydrographique et Océanographique de la Marine (S.H.O.M.). The year 1999, for which the most complete data base was available, was chosen as the reference simulation year, even if the *Ulva* biomass survey was done only in June 2000. Flow rates and

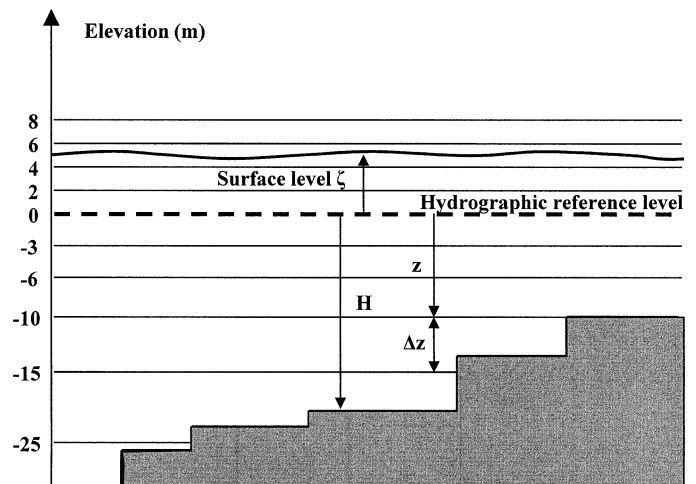


Fig. 4. Splitting the water column into layers referenced to the zero hydrographic level.

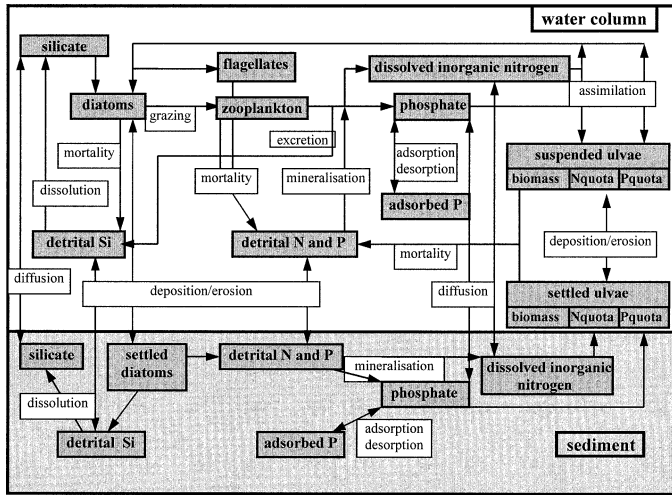


Fig. 5. Conceptual diagram of the biogeochemical part of the model.

nutrient concentrations in the tributaries were provided by the Brest municipal analysis laboratory. The MétéoFrance Brest-Guipavas meteorological station provided daily average measurements (sunshine duration, air temperature, air moisture, atmospheric pressure, cloud cover) or wind speed and direction every 3 h, which have been used for sea temperature and surface wind-induced stresses calculations. Seaward boundaries concentrations were not available for 1999; only 1993 values sampled by Le Pape et al. (1996) at the Iroise station (point I on Fig. 1) could be used.

Basic biogeochemical model of algal production—To be able to take into account the competition between phytoplankton and macroalgae in shallow eutrophicated zones, the biological submodel describes nitrogen, silicon, and phosphorus cycles. As the “nutrient > phytoplankton > zooplankton > detritus” path has been already fully described when used first in a spatial box model of the bay of Seine (Guillaud et al. 2000), then in a 3D model of the same area (Cugier et al. 2001; Cugier et al. 2005), only the new ingredients (*Ulva* components) will be detailed here. An overview of the structure of the whole biogeochemical model is shown in Fig. 5. The state variables of the basic model are described in Table 2. The differential equations summing up all the biogeochemical processes acting on the state variables are detailed in Web Appendix 1: http://www.aslo.org/lo/toc/vol51/issue_1_part2/0591a1.pdf. The parameters used in these equations are defined in Table 3.

In a classical fashion, *Ulva* growth rate is the product of a potential growth rate modulated by temperature and the minimum between respective light and nutrient limiting effects:

$$\mu = \mu_0 f_T \min(f_L, f_N),$$

where μ is *Ulva* growth rate (per day); μ_0 is *Ulva* potential growth rate extrapolated at 0°C (per day); f_T is temperature effect function; f_L is light effect function; f_N is nutrient effect function.

Table 2. State variables of the ecological model.

Symbol	Content
X_1	Ammonia
X_2	Nitrate
X_3	Dissolved silicon
X_4	Phosphate
X_5	Particulate exchangeable phosphorus
X_6	Diatom nitrogen
X_7	Flagellate nitrogen
X_8	Detrital organic nitrogen
X_9	Detrital biogenic silicon
X_{10}	Detrital organic phosphorus
X_{11}	Zooplankton nitrogen
X_{12}	Biomass of suspended ulvae
X_{13}	Nitrogen content of suspended ulvae
X_{14}	Phosphorus content of suspended ulvae
X_{15}	Biomass of settled ulvae
X_{16}	Nitrogen content of settled ulvae
X_{17}	Phosphorus content of settled ulvae

Temperature effect is considered as obeying a classical “ $Q_{10} = 2$ ” law in the range of 0–25°C:

$$f_T = \exp(k_t X_T)$$

where $k_t = 0.07^\circ\text{C}^{-1}$ (T in Celsius degrees).

Similarly to those of diatoms and dinoflagellates, the *Ulva* photosynthesis light curve is assumed to obey a Steele’s function (Steele 1962). For suspended ulvae, the light effect function is then:

$$f_{Lulvasusp} = \int_{z_{min}}^{z_{max}} \frac{I_z/2}{I_{optulva}} \exp\left(1 - \frac{I_z/2}{I_{optulva}}\right) dz$$

where $I_{optulva}$ is optimal light intensity for *Ulva* (W m^{-2}); I_z is total visible light intensity at depth z (W m^{-2}), considered as twice the PAR; z_{min} , z_{max} are depth of the ceiling and the floor of the water layer. For settled ulvae, the light effect function is a Steele’s formulation using directly the light available at the sea bottom I_H , and only for the superficial part of the deposit, considered as corresponding to a maximum biomass up to $b_{surfulva}$ (the excess of settled biomass is considered as being buried and, hence, in the dark).

$$f_{Lulvadep} = \frac{I_H/2}{I_{optulva}} \exp\left(1 - \frac{I_H/2}{I_{optulva}}\right)$$

Light intensity decreases with depth according to an exponential equation depending on a light extinction coefficient (K_z):

$$I_z = I_{surf} \exp(-K_z z),$$

where I_{surf} is surface light intensity (W m^{-2}).

The light extinction coefficient depends on suspended matter concentrations (Ménésguen et al. 1995), and on biomass of suspended ulvae:

$$K_z = k_1 X_{SM}^2 + k_{ulvasusp} X_{12},$$

where X_{SM} is suspended matter concentration (milligrams per liter) including mineral, detrital, and phytoplanktonic parti-

Table 3. Parameters of the biogeochemical model.

Symbol	Meaning	Unit	Value
Ulvae			
μ_{maxulva}	Maximum growth rate at 0°C	d ⁻¹	0.08
I_{optulva}	Optimal light intensity	W m ⁻²	60
K_{Nulva}	Half saturation constant for N uptake	μmol L ⁻¹	30
K_{Pulva}	Half saturation constant for P uptake	μmol L ⁻¹	5
V_{maxNulva}	Maximum N uptake rate	μmol g ⁻¹	200
V_{maxPulva}	Maximum P uptake rate	μmol g ⁻¹	30
q_{minN}	Minimum N : dry weight ratio	mg g ⁻¹	10
q_{maxN}	Maximum N : dry weight ratio	mg g ⁻¹	50
q_{minP}	Minimum P : dry weight ratio	mg g ⁻¹	1
q_{maxP}	Maximum P : dry weight ratio	mg g ⁻¹	4
m_{ulva}	Mortality rate at 0°C	d ⁻¹	0.01
b_{surfulva}	Surface specific biomass (dry weight)	kg m ⁻²	0.01
k_{ulvasusp}	Extinction coefficient for suspended ulvae	m ⁻¹ g ⁻¹ L	25
v_{cd}	critical deposition current velocity	m s ⁻¹	0.5
v_{ce}	critical erosion current velocity	m s ⁻¹	0.07
F_{ulva}	Flux of ulvae resuspended at $v = 2 v_{\text{ce}}$	mg m ⁻² s ⁻¹	0.1
W_{ulva}	Settling velocity	m d ⁻¹	500
Diatoms			
μ_{maxdiat}	Maximum growth rate at 0°C	d ⁻¹	0.45
I_{optdiat}	Optimal light intensity	W m ⁻²	100
K_{Ndiat}	Half saturation constant for N	μmol L ⁻¹	2
K_{Sidiat}	Half saturation constant for Si	μmol L ⁻¹	1
K_{Pdiat}	Half saturation constant for P	μmol L ⁻¹	0.15
v_{sdiatmin}	Minimal sedimentation velocity	m d ⁻¹	0.7
v_{sdiatmax}	Maximal sedimentation velocity	m d ⁻¹	2.1
m_{diat}	Mortality rate at 0°C	d ⁻¹	0.03
$r_{\text{Si:N}}$	Si : N ratio	mol mol ⁻¹	0.4
$r_{\text{P:N}}$	P : N ratio	mol mol ⁻¹	0.0625
$r_{\text{N:chloro}}$	N : chlorophyll <i>a</i> ratio	mol g ⁻¹	1
Dinoflagellates			
μ_{maxflag}	Maximum growth rate at 0°C	d ⁻¹	0.35
I_{optflag}	Optimal light intensity	W m ⁻²	170
K_{Nflag}	Half saturation constant for N	μmol L ⁻¹	3
K_{Pflag}	Half saturation constant for P	μmol L ⁻¹	0.10
m_{flag}	Mortality rate at 0°C	d ⁻¹	0.02
Zooplankton			
μ_{maxzoo}	Maximum growth rate at 0°C	d ⁻¹	0.3

Table 3. Continued.

Symbol	Meaning	Unit	Value
Ass	Assimilation	dimensionless	0.6
γ_{zoo}	Slope of Ivlev function	L μg ⁻¹	0.24
Pr_{th}	Chlorophyll predation threshold	μg L ⁻¹	2
e_{zoo}	Excretion rate	d ⁻¹	0.01
m_{minzoo}	Minimum mortality rate at 0°C	d ⁻¹	0.06
m_{tzoo}	Biomass dependent mortality rate at 0°C	d ⁻¹ μg ⁻¹ L	0.0006
$r_{\text{N:dwzoo}}$	N : dry weight ratio	μmol μg ⁻¹	0.0031
Particulate adsorbed phosphorus and detrital organic matter			
k_{desorp}	Phosphorus desorption rate	d ⁻¹	2.4
k_{adsorp}	Phosphorus adsorption rate	d ⁻¹ L μmol ⁻¹	0.12
Q_{0max}	Max. P adsorption capacity (suspended matter)	μmol g ⁻¹	7
k_{minN}	N mineralization rate at 0°C	d ⁻¹	0.05
k_{nitrif}	Nitrification rate at 0°C	d ⁻¹	0.2
k_{minP}	P mineralization rate at 0°C	d ⁻¹	0.1
k_{diss}	Si dissolution rate at 0°C	d ⁻¹	0.07
k1	First extinction coefficient for SM	m ⁻¹ mg ⁻¹ L	0.247
k2	Second extinction coefficient for SM	dimensionless	0.655

cles; and X_{12} is dry weight of suspended ulvae (grams per liter).

For diatoms as well as dinoflagellates, the nutrient (N, P, Si for diatoms) limitations on growth had been considered as following direct Michaelis–Menten kinetics of the nutrient concentrations in seawater:

$$f_{\text{N}} = \frac{\text{Nut}}{\text{Nut} + K_{\text{Nut}}}$$

where Nut is concentration in seawater for the nutrient under consideration (micromoles per liter) and K_{Nut} is half-saturation constant for the nutrient and phytoplankton group under consideration.

For *Ulva*, which is able to store important quantities of nitrogen and phosphorus, a more detailed representation of the growth process has been retained, using a modified version of the original cell quota model (Droop 1968). Nitrogen as well as phosphorus are taken up by *Ulva* biomass following Michaelis–Menten kinetics, and stored in the N or P internal pools of *Ulva*; the repletion state of these pools (i.e., the position of the nutrient cell quota q_{Nut} between its biological extrema q_{minNut} and q_{maxNut}) governs the nutrient limitation of the *Ulva* growth following another Michaelis–

Menten kinetics. The introduction of a maximum level of repletion, $q_{\max\text{Nut}}$, induces a necessary standardization of the original cell quota model formulation of the nutrient limiting factor, which becomes:

$$f_{\text{Nutulva}} = \frac{\frac{q_{\text{Nut}} - q_{\min\text{Nut}}}{q_{\text{Nut}}}}{\frac{q_{\max\text{Nut}} - q_{\min\text{Nut}}}{q_{\max\text{Nut}}}}$$

Similarly, it induces a weighting of the nutrient uptake velocity, which must vanish when the quota has reached its maximum value; as nitrate as well as phosphate uptake are light-dependent processes, the final nutrient uptake velocity becomes:

$$V_{\text{Nutulva}} = (I_z > 0)V_{\max\text{Nutulva}} \frac{\text{Nut}}{K_{\text{Nutulva}} + \text{Nut}} \left(\frac{q_{\max\text{Nut}} - q_{\text{Nut}}}{q_{\max\text{Nut}} - q_{\min\text{Nut}}} \right)$$

where I_z is the light intensity available at depth z , and $V_{\max\text{Nutulva}}$ and K_{Nutulva} the respective maximum uptake velocity and half-saturation constant for the nutrient concerned.

As for the phytoplanktonic algae, *Ulva* mortality (per day) is assumed to be temperature dependent: $m = m_{\text{ulva}} f_T$.

As in Brittany, and especially in the Bay of Brest, the *Ulva* biomass is made up of free-floating thalli; sedimentation of these suspended algae has to be taken into account, with a constant velocity, W_{ulva} (m s^{-1}). In the bottom layer, ulvae can settle on the sediment depending on the current velocity v , in a formulation derived from the Krone's one:

$$W_{\text{sedulva}} = \begin{cases} W_{\text{ulva}} \left(1 - \frac{v}{v_{\text{cd}}} \right) & \text{if } v_{\text{cd}} \geq v \\ 0 & \text{else} \end{cases}$$

where v = bottom current velocity, v_{cd} = critical deposition current velocity.

In the bottom layer, settled ulvae can be resuspended depending on the current velocity v , according to a formulation derived from the Partheniades one:

$$\text{Resusp}_{\text{ulvadep}} = \begin{cases} \frac{F_{\text{ulva}}}{X_{15}} \left(\frac{v}{v_{\text{ce}}} - 1 \right) & \text{if } v \geq v_{\text{ce}} \\ 0 & \text{else} \end{cases}$$

where v = bottom current velocity, v_{ce} = critical erosion current velocity, F_{ulva} = flux of ulvae resuspended at $v = 2v_{\text{ce}}$ ($\text{mg m}^{-2} \text{s}^{-1}$).

Additional equations for nutrient tracking—The method for assessing the fate of any quantitative property of a state variable in an ecological model has been already described by Ménésguen and Hoch (1997), when applied to the properties “age” and “birth place” of the state variables nitrate and diatoms: it consists in adding a copy of the advection–diffusion reaction equation of the carrying state variable, but applied to the product “carrying state variable \times carried property.” The time–space evolution of the carried property is then obtained by dividing this computed product by the carrying state variable.

Here we want to track the fate of the tributary signature, a conservative property (i.e., without any local source or sink, except at the boundaries), through the whole biogeochemical cycle of the element under concern (we make the assumption that all the processes exchanging matter with compartments not taken into account in the model are negligible in the area: e.g., N fixation or denitrification in the N cycle, definite burying of elements in deep sediment layers, etc.). For instance, if we want to follow in the marine ecosystem the nitrogen coming from the j th tributary, we must add a complete subset of differential equations dealing with all the nitrogenous state variables (eight in this model), applied now to the product “nitrogenous state variable \times proportion of nitrogen coming from the j th tributary.” When coupled to the transport equation, the following subset of eight differential equations, where Y_j is the name of the carried property “proportion of nitrogen coming from the j th tributary,” allows one to track the tagged nitrogen all over the ecological cycle and over the whole area of interest, including all possible recycling, that is to say whatever the time elapsed since the release of the tagged nitrogen in the marine ecosystem (provided the model has been run until steady state has been reached):

$\text{NH}_4\text{-N}$ coming from the j th tributary ($X_1 Y_j$) ($\mu\text{mol L}^{-1}$):

$$\begin{aligned} \frac{d(X_1 Y_j)}{dt} = & k_{\min\text{N}} f_T X_8 Y_j - \frac{X_1}{X_1 + X_2} Y_j \\ & \times \left\{ \mu_{\max\text{diat}} f_T \min(f_{\text{Ndiat}}, f_{\text{Sdiat}}, f_{\text{Pdiat}}, f_{\text{Ldiat}}) X_6 \right. \\ & + \mu_{\max\text{flag}} f_T \min(f_{\text{Nflag}}, f_{\text{Pflag}}, f_{\text{Lflag}}) X_7 \\ & + (I_z > 0) V_{\max\text{Nulva}} \frac{X_1 + X_2}{K_{\text{Nulva}} + X_1 + X_2} \\ & \times \left[\left(\frac{q_{\max\text{N}} - X_{13}/X_{12}}{q_{\max\text{N}} - q_{\min\text{N}}} \right) X_{12} \right. \\ & \left. \left. + \left(\frac{q_{\max\text{N}} - X_{16}/X_{15}}{q_{\max\text{N}} - q_{\min\text{N}}} \right) \frac{\min(b_{\text{surfulva}}, X_{15})}{z_{\max} - z_{\min}} \right] \right\} \\ & - k_{\text{nitri}} X_1 Y_j + e_{\text{zoo}} r_{\text{N/dwzoo}} f_T X_{11} Y_{j1} \end{aligned}$$

$\text{NO}_3\text{-N}$ coming from the j th tributary ($X_2 Y_j$) ($\mu\text{mol L}^{-1}$):

$$\begin{aligned} \frac{d(X_2 Y_j)}{dt} = & k_{\text{nitri}} X_1 Y_j - \frac{X_2}{X_1 + X_2} Y_j \\ & \times \left\{ \mu_{\max\text{diat}} f_T \min(f_{\text{Ndiat}}, f_{\text{Sdiat}}, f_{\text{Pdiat}}, f_{\text{Ldiat}}) X_6 \right. \\ & + \mu_{\max\text{flag}} f_T \min(f_{\text{Nflag}}, f_{\text{Pflag}}, f_{\text{Lflag}}) X_7 \\ & + (I_z > 0) V_{\max\text{Nulva}} \frac{X_1 + X_2}{K_{\text{Nulva}} + X_1 + X_2} \\ & \times \left[\left(\frac{q_{\max\text{N}} - X_{13}/X_{12}}{q_{\max\text{N}} - q_{\min\text{N}}} \right) X_{12} \right. \\ & \left. \left. + \left(\frac{q_{\max\text{N}} - X_{16}/X_{15}}{q_{\max\text{N}} - q_{\min\text{N}}} \right) \frac{\min(b_{\text{surfulva}}, X_{15})}{z_{\max} - z_{\min}} \right] \right\} \end{aligned}$$

Diatom nitrogen coming from the j th tributary ($X_6 Y_{j6}$) ($\mu\text{mol L}^{-1}$):

$$\begin{aligned} \frac{d(X_6 Y_{j6})}{dt} = & f_T \left[\mu_{\text{maxdiat}} \min(f_{\text{Ndiat}}, f_{\text{Sdiat}}, f_{\text{Pdiat}}, f_{\text{Ldiat}}) \right. \\ & \times \left(\frac{X_1}{X_1 + X_2} Y_{j1} + \frac{X_2}{X_1 + X_2} Y_{j2} \right) - m_{\text{diat}} Y_{j6} \left. \right] X_6 \\ & - \mu_{\text{maxzoo}} f_T \left\{ 1 - \exp \left[-\gamma_{\text{zoo}} \left(\frac{X_6}{r_{\text{N:chloro}}} - Pr_{\text{th}} \right) \right] \right\} \\ & \times r_{\text{N:dzwzo}} (X_{11} Y_{j11}) \end{aligned}$$

Flagellate nitrogen coming from the j th tributary ($X_7 Y_{j7}$) ($\mu\text{mol L}^{-1}$):

$$\begin{aligned} \frac{d(X_7 Y_{j7})}{dt} = & f_T \left[\mu_{\text{maxflag}} \min(f_{\text{Nflag}}, f_{\text{Pflag}}, f_{\text{Lflag}}) \right. \\ & \times \left(\frac{X_1}{X_1 + X_2} Y_{j1} + \frac{X_2}{X_1 + X_2} Y_{j2} \right) - m_{\text{flag}} Y_{j7} \left. \right] X_7 \end{aligned}$$

Detrital organic nitrogen coming from the j th tributary ($X_8 Y_{j8}$) ($\mu\text{mol L}^{-1}$):

$$\begin{aligned} \frac{d(X_8 Y_{j8})}{dt} = & m_{\text{diat}} f_T (X_6 Y_{j6}) + m_{\text{flag}} f_T (X_7 Y_{j7}) - k_{\text{Nmin}} f_T (X_8 Y_{j8}) \\ & + m_{\text{ulva}} f_T \left[X_{13} Y_{j13} + \frac{X_{16} Y_{j16}}{(z_{\text{max}} - z_{\text{min}})} \right] \\ & + f_T \max(m_{\text{minzoo}}, m_{\text{fzoo}} X_{11}) r_{\text{N:dzwzo}} (X_{11} Y_{j11}) \\ & + (1 - \text{Ass}) \mu_{\text{maxzoo}} \\ & \times f_T \left\{ 1 - \exp \left[-\gamma_{\text{zoo}} \left(\frac{X_6}{r_{\text{N:chloro}}} - Pr_{\text{th}} \right) \right] \right\} r_{\text{N:dzwzo}} X_{11} Y_{j6} \end{aligned}$$

Zooplankton biomass based on nitrogen coming from the j th tributary ($X_{11} Y_{j11}$) (mg m^{-3} dry weight):

$$\begin{aligned} \frac{d(X_{11} Y_{j11})}{dt} = & \mu_{\text{maxzoo}} \text{Ass} f_T \left\{ 1 - \exp \left[-\gamma_{\text{zoo}} \left(\frac{X_6}{r_{\text{N:chloro}}} - Pr_{\text{th}} \right) \right] \right\} \\ & \times X_{11} Y_{j6} - e_{\text{zoo}} f_T (X_{11} Y_{j11}) \\ & - f_T \max(m_{\text{minzoo}}, m_{\text{fzoo}} X_{11}) (X_{11} Y_{j11}) \end{aligned}$$

Nitrogen content of suspended ulvae coming from the j th tributary ($X_{13} Y_{j13}$) (g m^{-3}):

$$\begin{aligned} \frac{d(X_{13} Y_{j13})}{dt} = & 14 \times 10^{-3} (I_z > 0) V_{\text{maxNulva}} \frac{X_1 + X_2}{K_{\text{Nulva}} + X_1 + X_2} \\ & \times \left(\frac{q_{\text{maxN}} - X_{13}/X_{12}}{q_{\text{maxN}} - q_{\text{minN}}} \right) X_{12} \\ & \times \left(\frac{X_1}{X_1 + X_2} Y_{j1} + \frac{X_2}{X_1 + X_2} Y_{j2} \right) - m_{\text{ulva}} f_T (X_{13} Y_{j13}) \end{aligned}$$

$$+ \frac{\text{Resusp}_{\text{ulvade}}(X_{16} Y_{j16}) - \text{Wsed}_{\text{ulva}}(X_{13} Y_{j13})}{z_{\text{max}} - z_{\text{min}}}$$

Nitrogen content of settled ulvae coming from the j th tributary ($X_{16} Y_{j16}$) (g m^{-2}) (only in bottom layer):

$$\begin{aligned} \frac{d(X_{16} Y_{j16})}{dt} = & 14 \times 10^{-3} (I_z > 0) V_{\text{maxNulva}} \frac{X_1 + X_2}{K_{\text{Nulva}} + X_1 + X_2} \\ & \times \left(\frac{q_{\text{maxN}} - X_{16}/X_{15}}{q_{\text{maxN}} - q_{\text{minN}}} \right) \min(b_{\text{surf}} \text{ulva}, X_{15}) \\ & \times \left(\frac{X_1}{X_1 + X_2} Y_{j1} + \frac{X_2}{X_1 + X_2} Y_{j2} \right) \\ & - (m_{\text{ulva}} f_T + \text{Resusp}_{\text{ulvade}})(X_{16} Y_{j16}) \\ & + \text{Wsed}_{\text{ulva}}(X_{13} Y_{j13}) \end{aligned}$$

Every new nitrogen source we will want to track will generate an additional independent subset of eight differential equations of this form. Initial conditions for Y_{ji} fractions are set to zero all over the domain, and boundary conditions also are set to zero, except for the inorganic nutrient of interest in the j th tributary, which has permanently a boundary value $Y_j = 1$.

Results

Before detailing the *Ulva* compartment and its nitrogen supply, a few results will be given about the algal competitors of the *Ulva*, i.e., the two phytoplanktonic components, diatoms and flagellates. At the Sainte-Anne station (S.A point on Fig. 1), the only one where simultaneous time-series for nutrients and phytoplankton are available, but only at high tide, the simulation exhibits the seasonal pattern shown by the data, but only ammonia and chlorophyll can be considered as showing no systematic bias. Student's t -test performed on paired observed and simulated series gives a probability of 0.088 for ammonia and 0.035 for chlorophyll, i.e., compatible with the no-bias hypothesis at the 1% level. Simulated values for nitrate ($p = 10^{-7}$), silicate ($p = 0.0004$), and especially phosphate ($p = 10^{-12}$) appear to be regularly overestimated (Fig. 6), which is probably due to a lack of mixing in the river plumes. Although a calibration of vertical mixing has been done, on the basis of measured surface and bottom salinity maps of the Elorn estuary, the lack of high-frequency measurement of nutrients at every moment of the tide did not allow a finer tuning of vertical mixing; a small salinity discrepancy may induce quite a significant nutrient discrepancy due to the very high nutrient concentration in the freshwater source. Even if it is overestimated, the model shows the regular increase of nutrient concentrations every fortnight, especially in winter, when high tides allow river plumes to go further westward and reach the Sainte-Anne station; measures, systematically made at high tide, cannot capture the tidal oscillation of the concentrations, and are representative of the "marine" baseline of the nutrient concentration at the entrance of the bay. Figures 7 and 8 give the spatial distribution of the two phytoplanktonic components, diatoms and flagellates, at their

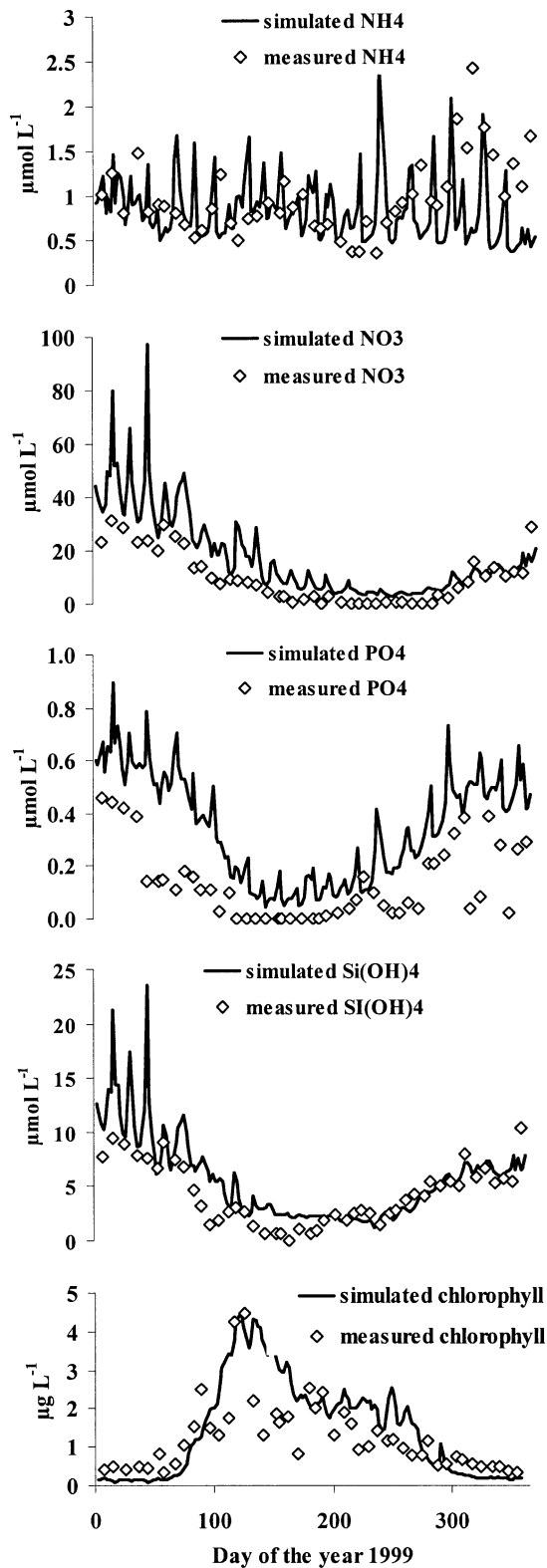


Fig. 6. Comparison between simulated and measured surface nutrients and chlorophyll at the Sainte-Anne station in 1999 (data from SOMLIT-Iroise monitoring station, Blain et al. 2004).

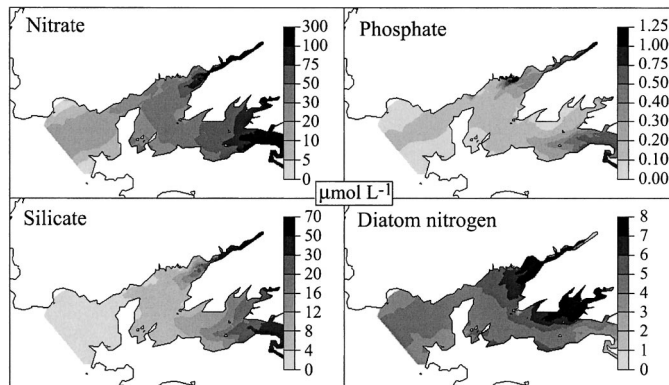


Fig. 7. Simulated surface distribution of nutrients and diatom nitrogen during the spring bloom peak.

respective yearly maximum: 1 May for diatoms and 30 September for dinoflagellates, along with the corresponding nutrient surface distributions. To be noticed is the difference between the northern (Elorn River), median (Daoulas River), and southern (Aulne River) estuaries, in terms of phytoplanktonic blooms: because of higher turbidity, the Aulne estuary is less favorable than the others to diatoms, whereas only the Elorn estuary is able to trigger a high summer bloom of dinoflagellates because of its sustained supply of nitrogen.

These first results, obtained with a 3D complete computation of instantaneous tidal flows reproducing the periodic variation of sea level, confirm the results previously obtained by the box model of Le Pape and Ménèsguen (1997), where tidal mixing was treated only as diffusive exchanges between boxes, at constant mean sea level. The strong vertical and horizontal mixing created twice a day by the oscillation of an important fraction of the water volume (ca. 12% during neap tides, 38% during spring tides) on both sides of the so-called Brest Channel succeeds in diluting and exporting the continuous nutrient terrestrial loading and the growing marine phytoplankton. This explains the paradoxical behavior of the Bay of Brest, i.e., the low level of phytoplankton biomass in the major part of the Bay despite the high nitrate loadings.

As far as macroalgal blooms are concerned, the use of

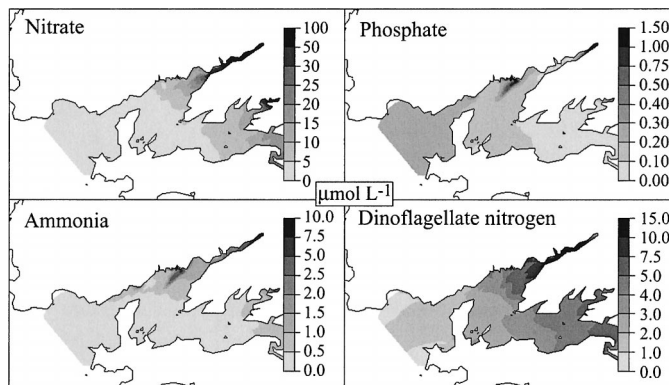


Fig. 8. Simulated surface distribution of nutrients and dinoflagellate nitrogen during the summer dinoflagellate peak.

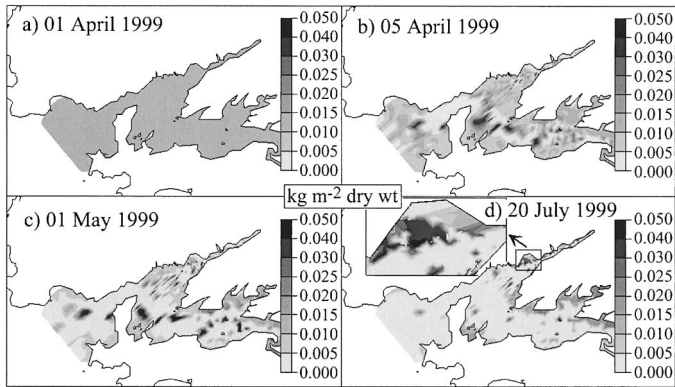


Fig. 9. Simulated time-course of settled ulvae in the Bay of Brest. (a) Imposed unrealistic uniform initial conditions at 1 April, (b) 5 d later, (c) 1 month later, and (d) at the annual maximum in the Moulin Blanc cove.

two *Ulva* compartments (suspended and settled) enhances the model robustness. Starting with a voluntarily unrealistic initial deposit of 10 g m^{-2} of *Ulva* on the bottom of the whole Bay of Brest, the model self-organizes in a realistic way, letting the *Ulva* stay and proliferate only in some embayments. As can be seen in the sequence of four images in Fig. 9, after a transitory phase of intense transport/deposition and decay, the model holds significant *Ulva* biomasses only in shallow waters near the shores where hydraulic trapping, light, and inorganic nitrogen availability are sufficient to allow a significant *Ulva* growth.

The place that spontaneously produces in the model the highest proliferation and accumulation of ulvae is the Moulin Blanc cove, with a maximum biomass deposit of about $270 \times 10^3 \text{ kg}$ of fresh weight, to be compared to the $400 \times 10^3 \text{ kg}$ actually measured in June 2000 by CEVA laboratory (Fig. 2).

The calculated contributions of the various sources of inorganic nitrogen (the rivers Elorn, Costour, Stang Alar, Aulne, the so-called Zone Industrielle Portuaire (ZIP) urban sewage plant, and the marine boundary) in the feeding of this green tide shows without ambiguity (see Fig. 10) the Elorn River as the main nitrogen provider of the green tide (about 50%); the ZIP urban sewage plant continuous load of ammonia provides up to 20% of algal nitrogen content during summer. The small rivers (Stang Alar and Costour) have a negligible effect, whereas the natural open sea brings ~15%.

The tracking technique also shows clearly that the nitrogen pool of the ulvae in the Moulin Blanc cove is totally renewed in 4 months (100% of *Ulva* nitrogen is labeled around day 210). This confirms that *Ulva* mass blooms are fundamentally annual, without memory from one year to the next, except as a very small inoculum, whether as thalli or as spores. Therefore, a response to a major decrease of total nitrogen loading should occur within a year.

A more classical approach of assessing the role of some tributaries in the global eutrophication has also been performed, using removal of various continental sources of nitrogen during the *Ulva* growth period, i.e., from April until November. As shown in Fig. 11, complete removal of dis-

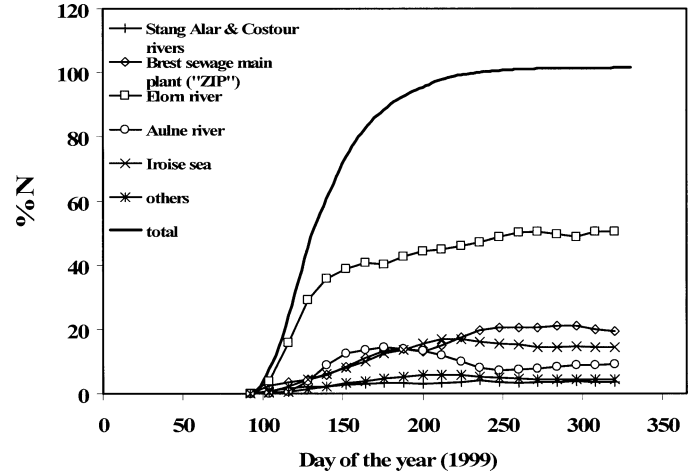


Fig. 10. Simulated accumulation of source markers in the nitrogen pool of settled ulvae in the Moulin Blanc cove area, as defined in the inset of Fig. 3.

solved inorganic nitrogen from all the tributaries of the Bay of Brest (except the Iroise Sea water entrance) would lead the first year to a weak *Ulva* spring bloom in the Moulin Blanc cove, followed by a rapid summer decline; continuing the simulation during a second year (not shown) does not produce any more significant *Ulva* biomass in the cove, because of the too-low overwintering *Ulva* biomass.

Discussion

The search for the importance of each source of nutrient loading in the observed cases of marine eutrophication is obviously of great operational concern, especially in the application of generalized restoration projects of water environments, as imposed in Europe by the Water Framework Directive (23 October 2000). Previous work clearly showed that nitrogen was the limiting nutrient in any case of *Ulva* proliferation (Ménésuegn 1992). Simulations performed with

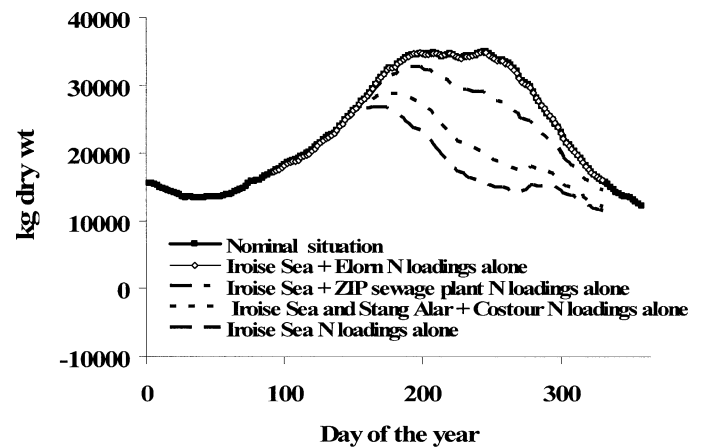


Fig. 11. Simulated time-course of total biomass of settled ulvae in the Moulin Blanc cove for scenarios of total removal of inorganic nitrogen in rivers, except in one of the three closest sources (Elorn, Stang Alar + Costour, ZIP sewage plant).

the present model have shown again the leading role of terrestrial nitrogen loading in *Ulva* blooming. Up to now, most published works on macrophyte eutrophication modeling have focused on reproducing the actual situation in a 0D manner (Coffaro and Sfriso 1997; Solidoro et al. 1997b; Martins and Marques 2002; Zaldivar et al. 2003), a multibox manner (Ménèsguen and Salomon 1988; Ménèsguen 1992; Runca et al. 1996; Bergamasco and Zago 1999), horizontal 2D manner (Salomonsen et al. 1999), or a 3D manner (Solidoro et al. 1997a). Some of them (Ménèsguen 1992; Runca et al. 1996; Solidoro et al. 1997a; Bergamasco and Zago 1999) have used their models to test the global effect of reducing nutrient loading, using the classical approach of diminishing the concentration of a specific source and comparing the modified situation to the nominal one. If this technique is the good one for simulating the expected effects of a particular remediation strategy, it cannot be used to measure the actual respective parts of the various sources in the present situation, because it alters the system and can deeply modify the balance between the actual sources. Especially in nutrient-saturated systems as the Bay of Brest, the simple removal of some sources, if not the main one, can lead to the erroneous conclusion that these sources have no role in the algal growth. Figure 11 shows for instance that the removal of all the sources, except the open sea entrance and the main river Elorn, doesn't change anything in the *Ulva* growth, whereas we can deduce from Fig. 10 that all these removed "secondary" sources actually supply up to 40% of the *Ulva* N demand! This illustrates how the tracking technique proposed here does not alter the system anyway, and allows really a "noninvasive auscultation" of the ecosystem. Another crucial advantage of our technique is to take into account the multitude of paths followed by an element in the ecosystem before its arrival in a specific compartment. For nitrogen for instance, an *Ulva* can take up nitrate coming directly from a tributary, but also ammonia excreted by zooplankton, having grazed phytoplankton grown on the nitrate coming from this tributary, or nitrate issued from the slow remineralization of dead ulvae buried in sediment, etc. In an attempt at a theoretical unfolding of food web networks, Higashi et al. (1989) introduced the notion of utilization coefficient n_{ij} as the total portion of the steady-state flow through compartment j that is ultimately experienced by consumer i . On the basis of a matrix approach of steady flows through a food web having possible recirculation paths, the Higashi et al. trophic network analysis aims at the same objective as our technique, but in pure biological food webs, free from physical constraints caused by their environment (e.g., transport by geophysical fluids) and considered at equilibrium. These restrictions allow the authors to develop an elegant algebraic Markov-type approach to the problem of finding the part of a resource arriving to a final consumer. Our introduction of the product "mass \times fraction of origin j ," which is a special case of the more general "carrying state variable \times carried property" product, allows a numerical generalization of this question to any unsteady food web embedded in a realistic environment. Moreover, our technique, which is of a eulerian type, allows tracking a chemical species or any property with exact mass conservation, even if it passes through different forms (e.g., different biogeo-

chemical compartments), whereas the classical lagrangian "particle tracking" technique is rather limited to single variables, without phase transitions, and does not furnish easily exact mass budgets in complex 3D ecosystem models.

References

- AUROUSSEAU, P. 2001. Les flux d'azote et de phosphore provenant des bassins versants de la rade de Brest. Comparaison avec la Bretagne. *Océanis* **27**: 137–161.
- BERGAMASCO, A., AND C. ZAGO. 2003. Exploring the nitrogen cycle and macroalgae dynamics in the lagoon of Venice using a multi-box model. *Estuar. Coast. Shelf Sci.* **48**: 155–175.
- BLAIN S., AND OTHERS. 2004. High frequency monitoring of the coastal marine environment using the MAREL buoy. *J. Environ. Monit.* **6**: 569–575.
- CEVA. 2000. Evaluation printanière des stocks immergés d'algues vertes en Rade de Brest (Moulin blanc, estuaire de l'Elorn). Rapport final pour la Communauté Urbaine de Brest.
- COFFARO, G., AND A. SFRISO. 1997. Simulation model of *Ulva rigida* growth in shallow water of the Lagoon of Venice. *Ecol. Model.* **102**: 55–66.
- CUGIER, P., AND P. LE HIR. 2000. Modélisation 3D des matières en suspension en baie de Seine Orientale (Manche, France). *C. R. Acad. Sci. Paris, Sciences de la Terre et des planètes* **331**: 287–294.
- , AND ———. 2002. Development of a 3D hydrodynamical model for coastal ecosystem modelling. Application to the plume of the Seine River (France). *Estuar. Coast. Shelf Sci.* **55**: 673–695.
- , A. MÉNESGUEN, AND J.-F. GUILLAUD. 2001. Modélisation écologique tridimensionnelle (3D) de la baie de Seine (Manche, France). *Hydroécol. Appl.* **13**: 21–35.
- , ———, AND ———. 2005. Three dimensional (3D) ecological modelling of the Bay of Seine (English Channel, France). *J. Sea Res.* **54**: 104–124.
- DROOP, M. R. 1968. Vitamin B12 and marine ecology, IV. The kinetics of uptake, growth and inhibition in *Monochrysis lutheri*. *J. Mar. Biol. Assoc. UK* **48**: 689–733.
- GUILLAUD, J.-F., F. ANDRIEUX, AND A. MÉNESGUEN. 2000. Biogeochemical modelling in the Bay of Seine (France): An improvement by introducing phosphorus in nutrient cycles. *J. Mar. Systems* **25**: 369–386.
- HIGASHI, M., T. P. BURNS, AND B. C. PATTEN. 1989. Food network unfolding: An extension of trophic dynamics for application to natural ecosystems. *J. Theor. Biol.* **140**: 243–261.
- HOWARTH, R. W., AND OTHERS. 1996. Regional nitrogen budgets and riverine N & P fluxes for the drainages to the North Atlantic Ocean: Natural and human influences. Nitrogen cycling in the North Atlantic Ocean and its watersheds. *Biogeochemistry* **35**: 75–139.
- LE PAPE, O., Y. DEL AMO, A. MÉNESGUEN, A. AMINOT, B. QUÉGUINER, AND P. TRÉGUER. 1996. Resistance of a coastal ecosystem to increasing eutrophic conditions: The Bay of Brest (France), a semi-enclosed zone of Western Europe. *Contin. Shelf Res.* **16**: 1885–1907.
- , AND A. MÉNESGUEN. 1997. Hydrodynamic prevention of eutrophication in the Bay of Brest (France): A modelling approach. *J. Mar. Systems* **12**: 171–186.
- MARTINS, I., AND J. C. MARQUES. 2002. A model for the growth of opportunistic macroalgae (*Enteromorpha* sp.) in tidal estuaries. *Estuar. Coast. Shelf Sci.* **55**: 247–257.
- MÉNESGUEN, A. 1992. Modelling coastal eutrophication: the case of French *Ulva* mass blooms. Proceedings of the International Conference on Marine Coastal Eutrophication. The response of

- marine transitional system to human impact: Problems and perspectives for restoration. 21–24 mars 1990, Bologne (Italie). *Sci. Total Environ.* (suppl.): 979–992.
- , J. F. GUILLAUD, A. AMINOT, AND T. HOCH. 1995. Modelling the eutrophication process in a river plume: the Seine River case study (France). *Ophelia* **42**: 205–225.
- , AND T. HOCH. 1997. Modelling the biogeochemical cycles of elements limiting primary production in the English Channel. I. Role of thermohaline stratification. *Mar. Ecol. Prog. Ser.* **146**: 173–188.
- , AND J.-C. SALOMON. 1988. Eutrophication modelling as a tool for fighting against *Ulva* coastal mass blooms, p. 443–450. *In* B. A. Schrefler and O. C. Zienkiewicz [eds.], *Computer modelling in ocean engineering*. Balkema.
- RUNCA, E., A. BERNSTEIN, L. POSTMA, AND G. DI SILVIO. 1996. Control of macroalgae blooms in the Lagoon of Venice. *Ocean Coast. Manage.* **30**: 235–257.
- SALOMONSEN, J., M. FLINDT, O. GEERTZ-HANSEN, AND C. JOHANSEN. 1999. Modelling advective transport of *Ulva lactuca* (L) in the sheltered bay, Møllekrogen, Roskilde Fjord, Denmark. *Hydrobiologia* **397**: 241–252.
- SCHINDLER, D. W. 1975. Whole-lake eutrophication experiments with phosphorus, nitrogen and carbon. *Verh. Internat. Verein. Limnol.* **1**: 3221–3231.
- SOLIDORO, C., V. E. BRANDO, C. DEJAK, D. FRANCO, R. PASTRES, AND G. PECENIK. 1997a. Long term simulations of population dynamics of *Ulva r.* in the lagoon of Venice. *Ecol. Model.* **102**: 259–272.
- , G. PECENIK, R. PASTRES, D. FRANCO, AND C. DEJAK. 1997b. Modelling macroalgae (*Ulva rigida*) in the Venice lagoon: Model structure identification and first parameters estimation. *Ecol. Model.* **94**: 191–206.
- SOUCHU, P. 1986. Contribution à l'étude de l'azote en écosystème macrotidal. Ph.D. thesis, Western Brittany University.
- STEELE, J. H. 1962. Environmental control of photosynthesis in the sea. *Limnol. Oceanogr.* **7**: 137–150.
- VOLLENWEIDER, R. A. 1968. The scientific basis of lake and stream eutrophication, with particular reference to phosphorus and nitrogen as eutrophication factors. Tech. Rep. OECD, Paris, DAS/DS1/68, 27.
- ZALDÍVAR, J. M., E. CATTANEO, M. PLUS, C. N. MURRAY, G. GIOR-DANI, AND P. VIAROLI. 2003. Long-term simulation of main biogeochemical events in a coastal lagoon: Sacca Di Goro (Northern Adriatic Coast, Italy). *Cont. Shelf Res.* **23**: 1847–1875.

Received: 12 March 2004

Accepted: 7 March 2005

Amended: 30 March 2005